Proceedings of IMECE2007
2007 ASME International Mechanical Engineering Congress and Exposition
November 11-15, 2007, Seattle, Washington, USA

IMECE2007-41565

FLOW PATTERN AND FRICTION COEFFICIENT OF WATER/NONADECANE-PARTICLE MIXTURE FLOW IN HORIZONTAL AND VERTICAL PIPES

Hiroya HASEGAWA, Chiba University
Chiba-shi, Inage-ku, Yayoi-cho 1-33, JAPAN

Makoto ONO, Chiba University
Chiba-shi, Inage-ku, Yayoi-cho 1-33, JAPAN

Makoto HISHIDA, Chiba University
Chiba-shi, Inage-ku, Yayoi-cho 1-33, JAPAN
(E-mail: hishida@faculty.chiba-u.jp)

Gaku TANAKA
Chiba-shi, Inage-ku, Yayoi-cho 1-33, JAPAN
(E-mail: gtanaka@faculty.chiba-u.jp)

ABSTRACT

Cold heat storage utilizing night-time electricity is one of the relevant technologies for the electric load leveling. Latent heat storage system with a large number of small paraffin particles is one of the promising technologies for the cold heat storage system. Small paraffin particles are generated by nozzle injection of liquid paraffin into cold water. Direct heat transfer between the ascending particles and surrounding cold water enhances the storage of latent heat in a short time. Transportation of solid paraffin particles suspended in water should be the best way to transport cold heat, because the density of cold heat stored in water/paraffin-particle mixture is very high. The present paper aims at investigating flow patterns and pressure loss of water/nonadecane-particle mixture flowing in horizontal and vertical pipes. The inner diameter and the average diameter of the nonadecane particle were 20mm and 3.7mm, respectively. Reynolds number, Froude number and volumetric concentration of nonadecane particles were varied in the ranges of $5000 \leq Re \leq 80000$, $1 \leq Fr \leq 260$ and $0.02 \leq Cv \leq 0.25$.We found the following main results:

(1) Four flow patterns were observed in the horizontal flow, (a) flow with a stationary particle bed, (b) flow with a sliding particle layer (c) heterogeneous suspension flow and (d) homogeneous suspension flow. The flow pattern shifted from (a) to (d) with increasing Reynolds number.
(2) Homogeneous suspension flow was observed in the vertical up-flow.
(3) Homogeneous and heterogeneous suspension flow was observed in the vertical down-flow.
(4) The pressure loss coefficients λ of the horizontal flow were correlated by a function of λ and Re ($\lambda = 0.479\,Re^{-0.311}$) for the heterogeneous and homogeneous suspension flows (Re≥about 25000) and by a function of the excess pressure loss coefficient Φ, Fr and Cv ($\phi / C_v^{0.58} = 72.4\,Fr^{-1.25}$) for the flow with a sliding particle layer (Re≤about 20000).
(5) The pressure loss coefficients of the vertical up-flow were correlated by a function of λ and Re ($\lambda = 4.45\,Re^{-0.501}$) in a large Reynolds number range of Re≥about 40000 and by a function of Φ, Fr and Cv ($\phi / C_v^{0.47} = 282\,Fr^{-1.47}$) in a small Reynolds number range of Re≤about 40000.
(6) The pressure loss coefficients of the vertical down-flow were correlated by a function of Φ and Fr ($\phi = 73.0\,Fr^{-0.765}$).

INTRODUCTION

Cold heat storage utilizing night-time electricity is one of the relevant technologies for the electric load leveling. Latent heat storage system with a large number of small paraffin particles is one of the promising technologies for the cold heat storage system [1]. Small paraffin particles are generated by nozzle injection of liquid paraffin into cold water. Direct heat transfer between the ascending particles and surrounding cold water enhances the storage of latent heat in a short time [2,3]. Transportation of solid paraffin particles suspended in water should be the best way to transport cold heat, because the density of cold heat stored in water/paraffin-particle mixture is very high.

Many studies have been carried out about hydraulic conveying of solid particles, for example coal, Perspex, sand and grave [4,5]. Flow patterns and pressure loss coefficients have been extensively investigated. However, only a few studies have been carried out about the hydraulic conveying of solid particles, like ice particles or paraffin particles, which are

relevant to the cold heat transportation. The characteristic of the hydraulic conveying of ice or paraffin particles is that the density of the particle is very close to water or lighter than water. Shirakashi et al. [6] investigated flow pattern and pressure loss of the water/polypropylene-particle (density =900kg/m^3) mixture flowing in a horizontal pipe and they proposed an empirical correlation for the excess pressure loss coefficient. They pointed out that the pressure loss decreases in a small range of the volumetric concentration of particles. Bnadoh et al. [7] examined flow pattern and pressure loss of a horizontal, vertical up- and vertical down-flow in which water/polypropylene-particle (density =910kg/m^3) mixture was flowing. Shirakashi et al. [8], Onojima et al. [9], Kawanami et al. [10] and Horibe [11] studied flow pattern and pressure loss of water/ice or water/snow mixture flowing in a horizontal and vertical pipe. However, only little studies have been carried out to investigate hydraulic conveying of solid particles whose density is lighter than water, and it seems that there has not been established the correlation that can predict the pressure loss of water/paraffin-particle mixture flowing in the horizontal and vertical pipe.

The present paper aims at investigating flow patterns and pressure loss of horizontal flow, vertical up-flow and vertical down-flow of water/nonadecane-particle mixture.

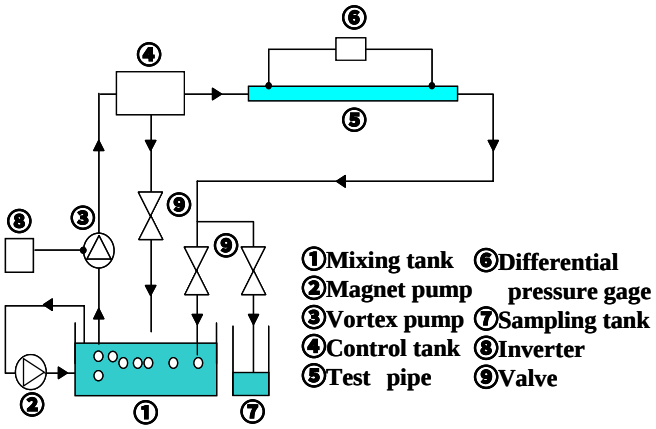

Fig.1 Experimental setup

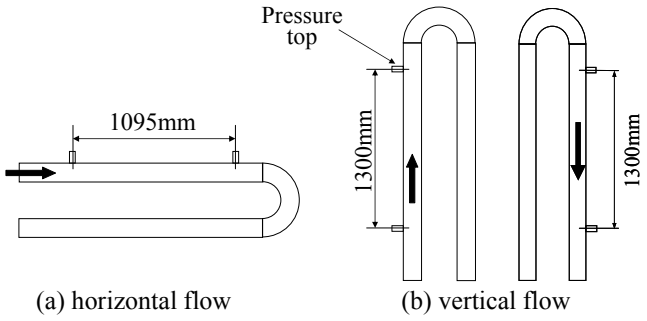

Fig.2 Test pipe for horizontal and vertical flow

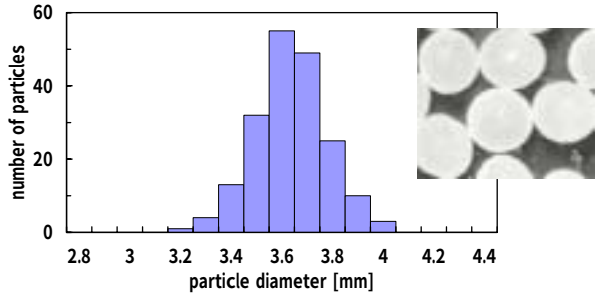

Fig.3 Distribution of particle diameter

EXPERIMENTAT SETUP AND PROCEDURE

Figure 1 shows present experimental setup which was comprised of a mixing tank, magnet pump, vortex pump, control tank, test pipe and measuring devices for pressure drop, flow rate of water/nonadecane-particle mixture and concentration of nonadecane particles.

The mixing tank contained water and nonadecane particle mixture the particle concentration of which was kept uniform by circulating water with the magnetic pump. The vortex pump supplied the test pipe with water/nonadecane-particle mixture. The flow rate of the mixture was varied by changing the rotation of the vortex pump by means of an inverter. The control tank had four side branch pipes which were able to return only water back to the mixing tank. By controlling the flow rate of water through the side branch pipes to the mixing tank the concentration of nonadecane particles at the inlet of the test pipe was fixed at a constant value. The acrylic test pipe had an inner diameter of 20mm, outer diameter of 26mm and a length of 3000-4000mm. The pressure taps were drilled in the wall of test pipe to measure the pressure drop through the straight test pipe. The distance between two pressure taps was 1095-1300mm. A differential pressure gage and a manometer were used for measuring the pressure difference between the two pressure taps. The flow rate of the mixture was determined by measuring the time required for the mixture to fill a volume-measuring sampling tank. The concentration of nonadecane particles was determined by measuring the volume of particles collected in the volume-measuring sampling tank. The main flow was temporally switched to the volume-measuring sampling tank to measure the flow rate of the mixture and the concentration of particles. Flow pattern of the mixture was visualized by a high speed video camera.

In the present experimental study investigated were the pressure drop and the flow pattern for horizontal flow, vertical up-flow and vertical down-flow through the straight round test pipe. Figure 2(a)(b) show schematic drawing of the test pipes. The pressure taps were fixed on the upper side of the round pipe. We had no problem for measuring the pressure, because the inner diameter of the pressure taps was so small (=1mm) that no nonadecane particles blocked the pressure taps.

Nonadecane particles used for the present experiment had an average diameter of 3.7mm and their distribution of diameter is shown in Figure 3. The melting temperature and

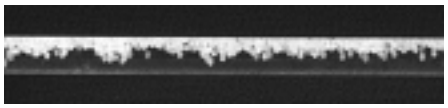

(a) flow with a stationary particle bed (Re=2400, C_v=-----)

(b) flow with a sliding particle layer (Re=8560, C_v=0.084)

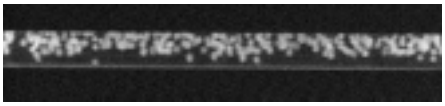

(c) heterogeneous suspension flow (Re=28500, C_v=0.070)

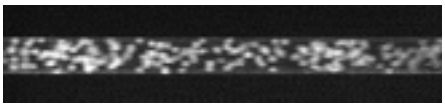

(d) homogeneous suspension flow (Re=63000, C_v=0.079)

Fig.4 Flow patterns observed in horizontal flow

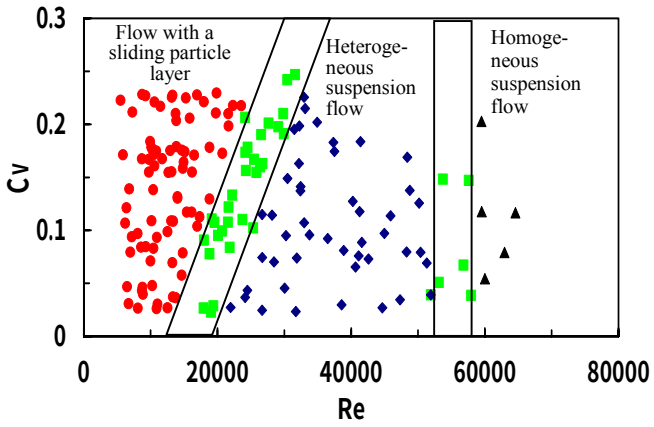

Fig.5 Flow patterns observed in horizontal flow

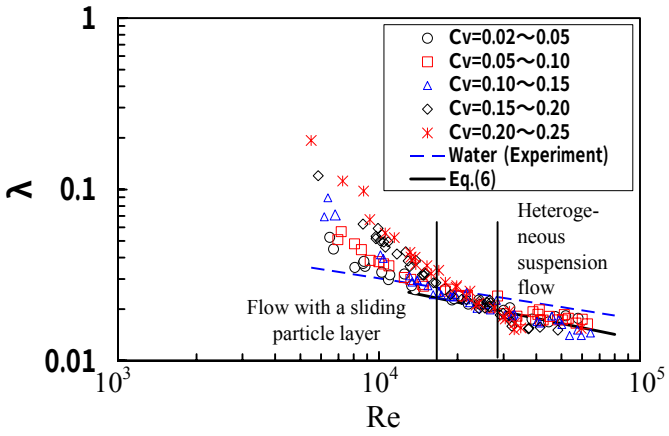

Fig.6 Plots of λ against Re for horizontal flow

density of nonadecane were 31.3˚C and 0.788kg/m^3, respectively. Reynolds number Re and Froude number Fr (Equation 2) were ranged from 5000 to 80000 and from 1 to 260, respectively, by varying the average velocity U_m of the water/nonadecane-particle mixture from 0.2 to 3.5 m/s.

$$Re = U_m \cdot d / \nu_w \quad (1)$$

$$Fr = U_m^2 /(gd|s-1|) \quad (2)$$

Here, d, ν_w, g and s are the inner diameter of the test pipe, dynamic viscosity of water, acceleration of gravity and specific gravity of nonadecane, respectively.

The pressure loss coefficient λ was calculated by

$$\lambda_m = \Delta P_m \frac{d}{L}\frac{2}{\rho_m U^2} \quad (3),$$

$$\Delta P_m = \Delta P_0 + (\rho_w - \rho_m) gL \cdot \sin\varphi \quad (4),$$

where L and φ are the distance of the two pressure taps and inclination angle of the test pipe ($\varphi = 0$ for the horizontal flow and $\varphi = 90°$ for the vertical flow). ΔP_0 is the reading of the differential pressure on the difference pressure gauge. ρ_w and ρ_m are density of water and the mixture, respectively.

The volumetric concentration of nonadecane particles C_v measured at the exit of the test pipe was calculated by

$$C_v = \frac{V_n}{V_n + V_w} = \frac{W_n / \rho_n}{(W_n / \rho_n + W_w / \rho_w)} \quad (5),$$

where V, W and ρ are the volume, weight and density of particles and water collected in the volume-measuring sampling tank. Subscripts n and w indicate nonadecane and water.

EXPERIMENTAT RESULTS

Horizontal flow

Figure 4 shows various flow patterns observed in the horizontal flow. At low velocities particles tended to collect at the top of the pipe and formed a stationary particle bed. At higher velocities the mixture flow took the form of fully-suspended flow, though the concentration of particles in a vertical direction was uniform or not uniform. Four distinct flow patters were observable as shown in Figure 4:

(a) stationary bed of particles with suspended flow at the interface with water flow
(flow with a stationary particle bed, Figure 4(a));
(b) sliding layer of particles with or without suspended flow at the interface with water flow
(flow with a sliding particle layer, Figure 4(b));
(c) fully suspended flow with non-uniform particle concentration in the vertical direction
(heterogeneous suspension flow, Figure 4(c)); and
(d) fully suspended flow with uniform particle concentration
(homogeneous suspension flow, Figure 4(d)).

These flow patterns occurred successively with increasing velocity for any given particle concentration. In Figure 5, an attempt has been made to define the flow regimes. Flow patters

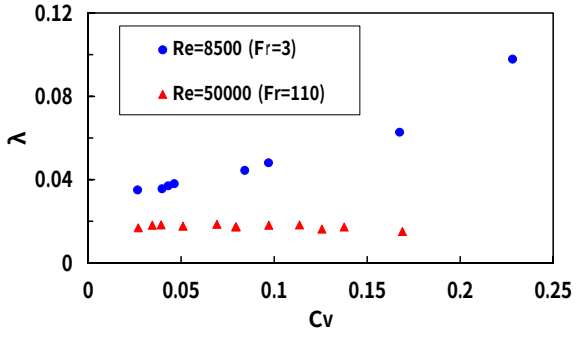

Fig.7 Plots of λ against C_v (Re=8500, 50000)

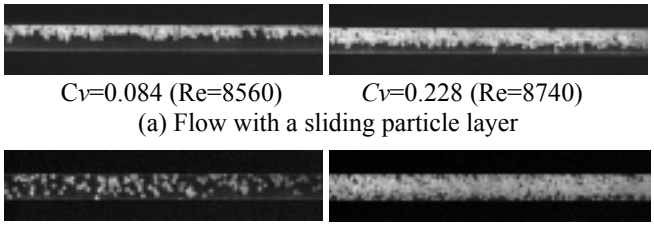

Cv=0.084 (Re=8560) *Cv*=0.228 (Re=8740)

(a) Flow with a sliding particle layer

Cv=0.051 (Re=53100) *Cv*=0.249 (Re=48800)

(b) Heterogeneous suspension flow

Fig.8 (a) Change of thickness of the sliding particle layer with *Cv*, (b) suspension flow for a small and large *Cv*

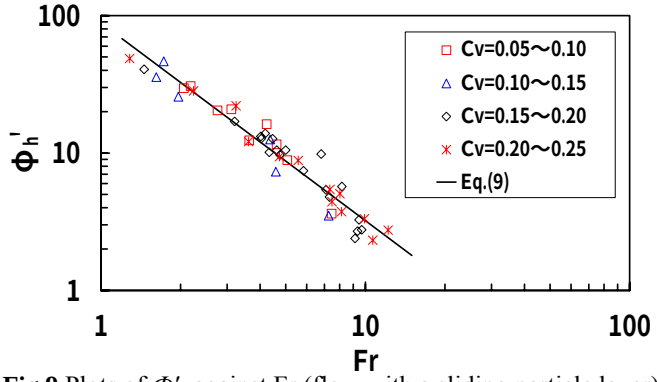

Fig.9 Plots of Φ'_h against Fr (flow with a sliding particle layer)

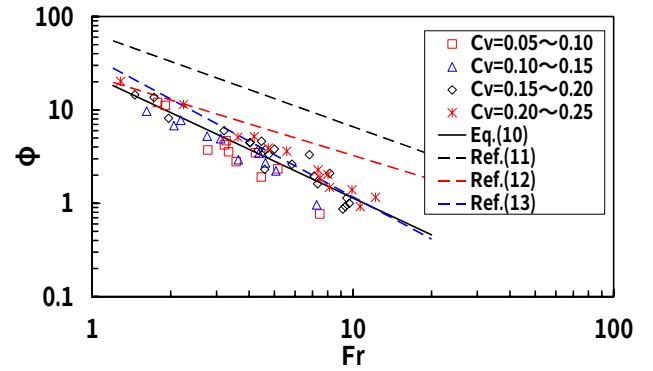

Fig.10 Comparison of Φ (flow with a sliding particle layer)

seemed to vary depending strongly on Reynolds number. At high concentrations the boundary between the heterogeneous flow and the flow with a sliding particle layer tended to shift toward higher Re.

In Figure 6 pressure loss coefficients are plotted against Reynolds number. A dotted straight line in the figure represents the correlation of measured friction loss coefficient for water flow (single phase flow). It will be seen that the pressure loss coefficients for the heterogeneous and homogeneous suspension flows in the Reynolds number range of Re≥about 25000 seemed to exhibit the same value irrespective of particle concentration. They were correlated by

$$\lambda = 0.479\, Re^{-0.311} \qquad (6).$$

It will be interesting to note that the pressure loss coefficients of the heterogeneous and homogeneous suspension flows were less than those of the water single phase flow. The same characteristic of the pressure loss reduction was reported by many researchers. For example, Shirakashi et al. [6] reported experimental results of the pressure loss reduction examined in the water/plastic-bead mixture flow. The density of the plastic-beads was 1040 and 900 kg/m^3 and the equivalent diameter of which was 3.06mm and 0.77mm.

Triangular symbols in Figure 7 indicates that the pressure loss coefficients of the suspension flow (Re=50000) remained at the same value in the present experimental range 0.02≤ *Cv* ≤0.25. In this *Cv* range the flow pattern remained the same (suspension flow) irrespective to the volumetric concentration as shown in Figures 8 and 5.

Pressure loss coefficients for the flow with a sliding particle layer in the Reynolds number range of Re≤20000, on the contrary, varied depending on the volumetric concentration *Cv*. Circular symbols in Figure 7 show that the pressure loss coefficient of the flow with a sliding particle layer (Re=8500) increased with increasing the volumetric concentration C_v. This will be explained by the fact that the thickness of the sliding particle layer (or the number of sliding particles) increased with increasing C_v as is suggested by the flow visualization results shown in Figure 8. The sliding particles traveled with lower velocity than water and produced additional pressure loss besides the friction loss of the water flow.

Figure 9 is a trial to correlate the pressure loss of the flow with a sliding particle layer as a function of the excess pressure loss coefficient Φ and the volumetric concentration *Cv* and Froude number Fr. Φ is defined by

$$\phi = (i_m - i_w)(C_v \cdot i_w) \qquad (7),$$

$$i_m = \Delta P_m / (L \cdot \rho_w g), \qquad i_w = \Delta P_w / (L \cdot \rho_w g) \qquad (8),$$

where $\Delta P_m / L$ and $\Delta P_w / L$ are the pressure gradient for the water/nonadecane-particle mixture flow and the water flow (single phase flow). The measured pressure loss of the flow with a sliding particle layer was well correlated by Equation (9).

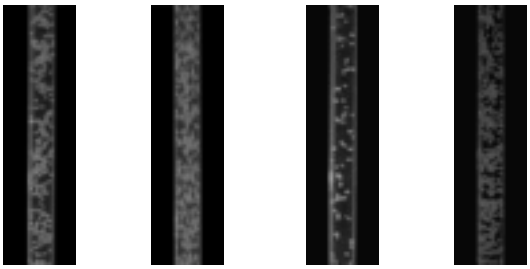

(a) Re=15000 (b) Re=58300 (c) Re=15700 (d) Re=15000
Cv=0.103 *Cv*=0.124 *Cv*=0.035 *Cv*=0.192

Fig.11 Flow patterns observed in vertical up-flow

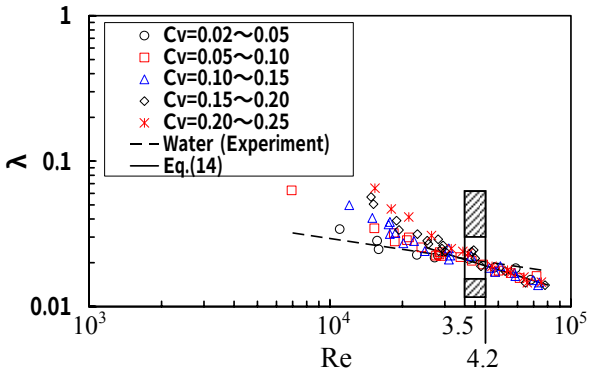

Fig.12 Plots of λ against Re for vertical up-flow

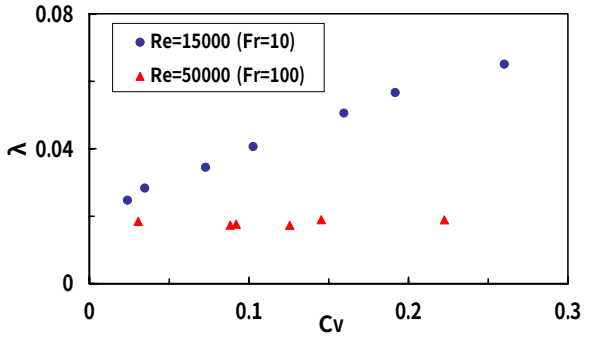

Fig.13 Plots of λ against C_v (Re=15000, 50000)

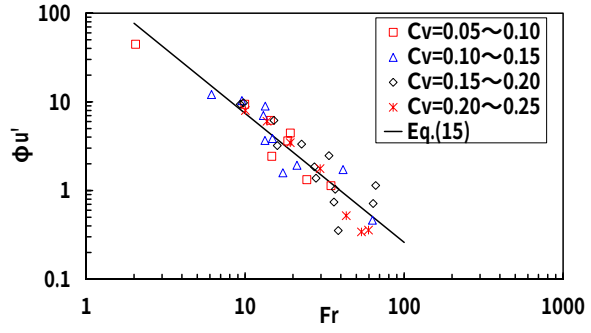

Fig.14 Plots of Φ'_u against Fr (Re<about 40000)

$$\phi'_h = \phi / C_v^{0.58} = 72.4 Fr^{-1.25} \quad (9)$$

It may be interesting to compare the present excess pressure loss coefficient of the flow with a sliding particle layer with existing empirical correlations. Only for the purpose of comparison with the empirical correlations proposed by other researchers, if the present pressure loss data of the flow with a sliding particle layer were correlated by a function between the excess pressure loss coefficient Φ and Froude number Fr, Equation 10 may be obtained. It, however, should be mentioned that correlating the present data by the function between Φ and Fr does not seem to be appropriate, because the present excess pressure loss coefficient Φ increased with increasing *Cv*.

$$\phi = 22.7 Fr^{-1.27} \quad (10)$$

Figure 10 compares the present experimental data shown by symbols with the correlations proposed by Newitt et al. [4] for water mixed with coal, or MnO_2 or gravel particles, Onojima H. et al. [9] for water-ice mixture and Miyae. [12] for water-beach sand mixture. They are represented by

$$\phi = 66 \cdot Fr^{-1} \quad (11)[4],$$

$$\phi = 20 \cdot Fr^{-0.8} \quad (12)[9],$$

$$\phi = 37 \cdot Fr^{-3/2} \quad (13)[12].$$

Vertical up- flow

Figure 11 shows that the vertical up-flow exhibited the same flow pattern, homogeneous suspension flow, in the whole present experimental ranges of Reynolds number 6000≤Re≤ 80000 and the volumetric concentration of particle 0.02≤*Cv*≤0.25.

Figure 12 plots the pressure loss coefficient λ of the vertical up-flow against Reynolds number Re. A dotted straight line in the figure represents the correlation of measured friction loss coefficient for water flow (single phase flow). It will be seen that the pressure loss coefficients in a large Reynolds number range Re≥about 40000 varied depending only on Reynolds number and they held the same value irrespective of the volumetric concentration *Cv*. They were correlated by

$$\lambda = 4.45\, Re^{-0.501} \quad (14).$$

Triangular symbols in Figure 13 represent the pressure loss coefficient for a large Reynolds number (Re=50000). They remained the same value in the whole range of 0.02≤*Cv*≤0.25.

Pressure loss coefficients in a small Reynolds number range of Re≤about 40000, on the other hand, increased with increasing *Cv* as shown in Figures 12 and 13 (circular symbols). It seems strange and interesting that the pressure loss coefficient increased with increasing *Cv*. We need further investigation to explain the experimental results.

Figure 14 correlates the pressure loss of the vertical up-flow in the small Reynolds number range (Re≤about 40000). The present experimental results were well correlated by

$$\phi'_u = \phi / C_v^{0.47} = 282 Fr^{-1.47} \quad (15).$$

Vertical down- flow

The vertical down-flow exhibited two flow patterns, heterogeneous and homogeneous suspension flows. Figure 15(a) and (c) show that particles tended to gather in the central area of the pipe and formed heterogeneous suspension flow at low velocities, while Figure 15(b) and (d) indicate that at high velocities particles dispersed uniformly in the entire flow region of the pipe and formed the homogeneous suspension flow. The shift of flow pattern from heterogeneous suspension to homogeneous suspension occurred gradually with increasing velocity.

(a) Re=15500 *Cv*=0.121 (b) 60700 *Cv*=0.137 (c) 15000 *Cv*=0.091 (d) 15300 *Cv*=0.214

Fig.15 Flow patterns observed in vertical down-flow

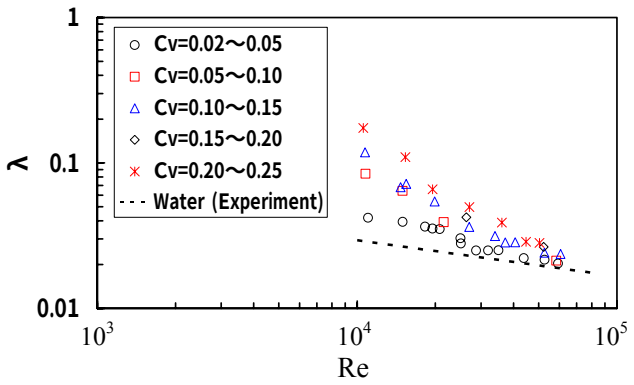

Fig.16 Plots of λ against Re for vertical down-flow

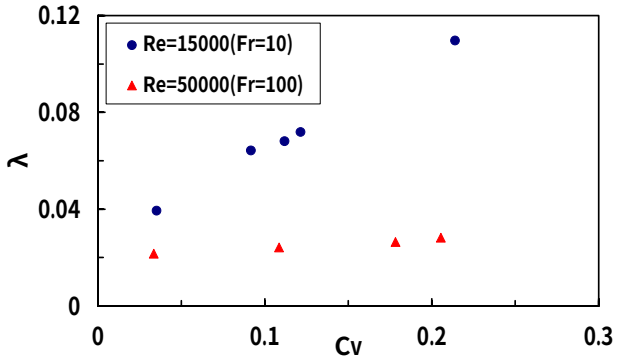

Fig.17 Plots of λ against C_v (Re=15000, 50000)

Figure 16 shows plots of the pressure loss coefficient λ of the vertical down-flow against Reynolds number Re. A dotted straight line in the figure represents the correlation of measured friction loss coefficient for water flow (single phase flow).

Figure 17 demonstrates that the pressure loss coefficients in the present Reynolds number range of $10000 \leq Re \leq 61000$ increased with increasing the volumetric concentration, though the dependency of λ on Cv became less with increasing Re.

Figure 18 correlates the pressure loss of the vertical down-flow in terms of the excess pressure loss coefficient Φ and Froude number Fr. The present experimental results were well correlated by

$$\phi = 73.0 Fr^{-0.765} \qquad (16).$$

Comparison of pressure loss between horizontal flow, vertical up-flow and vertical down- flow

Figure 19 compares the pressure loss coefficients between the horizontal flow, vertical up-flow and vertical down-flow (the volumetric concentration Cv=0.10-0.15). The vertical down-flow had the largest pressure loss coefficient, and the vertical up-flow the second largest one, and the horizontal flow had the smallest one.

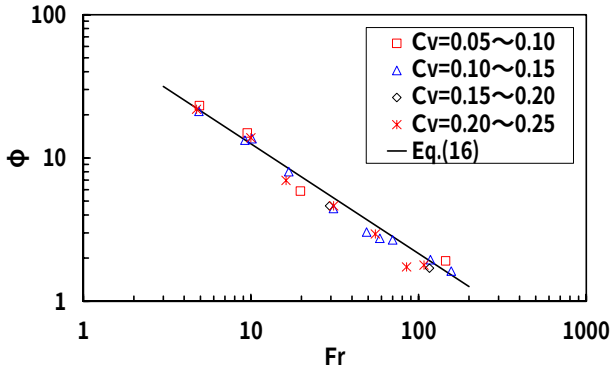

Fig.18 Plots of Φ against Fr

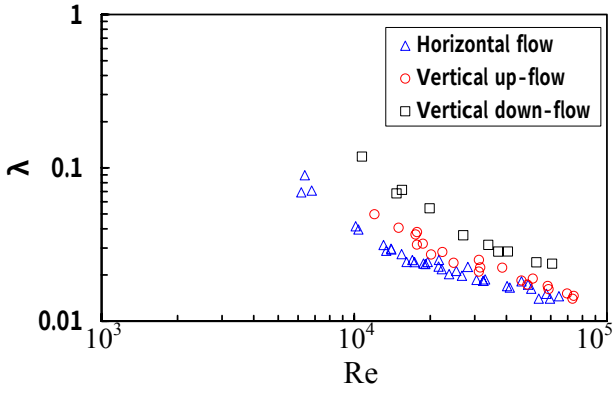

Fig.19 Comparison of λ between horizontal flow, vertical up-flow and vertical down-flow (Cv=0.10-0.15)

It seems interesting and strange that the pressure loss coefficient of the vertical up-flow was greater than that of horizontal flow. We need further investigations to explain the experimental results.

CONCLUSION

Flow pattern of water/nonadecane-particle mixture flow was observed and the pressure loss coefficient was measured for the horizontal flow, vertical up-flow and vertical down-flow which were flowing in a straight pipe with an inner diameter of 20mm. Reynolds number, Froude number and volumetric concentration of nonadecane particles were varied in the ranges of 5000≤ Re ≤80000, 1≤ Fr ≤ 260 and 0.02 ≤ Cv ≤ 0.25.

We found the following main results:

(1) Four flow patterns were observed in the horizontal flow, (a) flow with a stationary particle bed, (b) flow with a sliding particle layer (c) heterogeneous suspension flow and (d) homogeneous suspension flow. The flow pattern shifted from (a) to (d) with increasing Reynolds number.

(2) Homogeneous suspension flow was observed in the vertical up-flow

(3) Homogeneous and heterogeneous suspension flow was observed in the vertical down-flow.

(4) The pressure loss coefficients of the horizontal flow were correlated by $\lambda = 0.479\,Re^{-0.311}$ for the heterogeneous and homogeneous suspension flows (Re≥about 25000) and by $\phi / C_v^{0.58} = 72.4 Fr^{-1.25}$ for the flow with a sliding particle layer (Re≤about 20000). The pressure loss coefficient of the flow with a sliding particle layer increased with increasing the volumetric concentration of particles, while that of the suspension flow remained the same irrespective to Cv.

(5) The pressure loss coefficients of the vertical up-flow were correlated by $\lambda = 4.45\,Re^{-0.501}$ in a large Reynolds number range of Re≥about 40000 and by $\phi / C_v^{0.47} = 282 Fr^{-1.47}$ in a small Reynolds number range of Re≤about 40000. The pressure loss coefficient in the small Reynolds number range increased with the volumetric concentration of particles.

(6) The pressure loss coefficients of the vertical down-flow were correlated by $\phi / C_v^{0.834} = 45.6 Fr^{-0.766}$.

(7) The vertical down-flow had the largest pressure loss coefficient, and the vertical up-flow the second largest one, and that of the horizontal flow had the smallest one.

ACKNOWLEDGMENTS

This research was supported in part by the Grant-in-Aid for Scientific Research (C) (No.17560170) of Japan Society for the Promotion of Science.

REFERENCES

[1] INABA H. and SATO K., 1994, "Fundamental study on latent cold heat storage by means of oil droplets with low freezing point (1st report)", Trans. JSME, 60, No.580B, pp.4236-4243.

[2] INABA H. and SATO K., 1996, "Fundamental study on latent cold heat storage by means of oil droplets with low freezing point (2nd report)", Trans. JSME, 60, No.580B, pp.4236-4243.

[3] NAKAO Y., TANAKA G. and HISHIDA M., 2004, "Solidification characteristics of rising immiscible oil droplets in refrigerant solution", Trans. JSME, 70, No.691B, 758-766.

[4] NEWITT M.C., RICHARDSON J.F., ABBOTT M. and TURTLE R.B., 1955, "Hydraulic conveying of solids in horizontal pipes", Trans. Instn Chem. Engrs, 33, pp.93-113.

[5] MORIKAWA T., Liquid/solid two phase flow–transportation by air and water-, The nikkan kogyo shinbun, LTD.

[6] SHIRAKASHI M., TOKUNAGA Y. and HASHIMOTO T., 2004, "Pressure loss reduction due to mixing of coarse particles", Trans. JSME, 53, No.490B, pp.1672-1676.

[7] BANDO Y., FUJIMORI K., NAKAMURA M., SUZUKI M. and YOSHITOSHI K., 1998, "Flow characteristics for solid-liquid two phase flow using particles with lower density than that of liquid", Kagakukogaku Ronbunshu, 24, No.1, pp.138-139.

[8] SHIRAKASHI M., KAWADA Y. and TAKAHASHI S., 1995, "Characteristics of ice/water mixture in horizontal circular pipes", Trans. JSME, 61, No.585B, pp.1632-1639.

[9] ONOJIMA H., FUKUSHIMA M. and TSUBOTA Y., 1999, "Pressure loss of the ice/water mixture in the horizontal and vertical pipings, Studies on the ice/water mixture transportation for HVAC systems Part 1" J. Archit. Plann. Eng., AIJ, No.519, pp.63-68.

[10] KAWANAMI T., YAMADA M., IKEGAWA M. and TANABE W., 2003, "Flow characteristics and heat transfer of ice slurries", 40th National Heat Transfer Symposium of Japan, D211, 423-424.

[11] HORIBE A., 2006, "Flow and heat transfer characteristics of latent heat storage materials mixture such as ice slurries", Proceedings of 2006 JSRAE Annual Conference, A301, pp.491-494

[12] MIYAE S., 1974, "Optimum transportation condition for hydraulic conveying of solid particles", Trans. JSME, 40, No.333[2], pp.1321-1330.